

# The reactions $pn \rightarrow d\omega$ and $pn \rightarrow d\phi$ near threshold

K. Nakayama<sup>a,b</sup>, J. Haidenbauer<sup>b</sup>, and J. Speth<sup>b</sup>

<sup>a</sup>*Department of Physics and Astronomy, University of Georgia, Athens, GA 30602, USA*

<sup>b</sup>*Institut für Kernphysik, Forschungszentrum Jülich GmbH, D-52425 Jülich, Germany*

## Abstract

The reactions  $pn \rightarrow d\omega$  and  $pn \rightarrow d\phi$  are studied within a relativistic meson-exchange model of hadronic interactions. Predictions for the total cross sections and for the angular distributions of the vector mesons are presented. The resulting cross sections near threshold are around 10 - 30  $\mu\text{b}$  for  $pn \rightarrow d\omega$  and 200 - 250 nb for  $pn \rightarrow d\phi$ . A moderate deviation of the cross section ratio  $\sigma_{pn \rightarrow d\phi}/\sigma_{pn \rightarrow d\omega}$  from that of the Okubo-Zweig-Iizuka rule is predicted.

PACS: 13.75.-n, 14.20.Dh, 25.10+s, 25.40-h

## I. INTRODUCTION

The possibility that there might be a rather significant strangeness content in the nucleon, as indicated by the analysis of the  $\pi$ -nucleon  $\Sigma$  term [1] and the lepton deep-inelastic scattering data by the EMC and successor experiments [2], has triggered a wealth of experimental and theoretical investigations on this topic over the last decade. In this context, hadronic reactions at low and medium energy play an important role. Here one expects that the presence of strangeness in the nucleons would manifest itself in counting rates that significantly exceed predictions based on the Okubo-Zweig-Iizuka (OZI) rule [3,4]. Indeed, the experiments on antiproton-proton ( $\bar{p}p$ ) annihilation at rest at the LEAR facility at CERN revealed a strong violation of the OZI rule for various decay channels involving the  $\phi$  meson [5–7]. Substantial deviations from the OZI rule were also found in the reactions  $pd \rightarrow {}^3\text{He}\phi$  [8] and  $\bar{p}p \rightarrow \phi\phi$  [9]. More recently the DISTO collaboration reported on an experiment on exclusive production of  $\phi$  and  $\omega$  mesons in proton-proton ( $pp$ ) collisions [10]. In this measurement a cross section ratio of about a factor 10 larger than the estimate from the OZI rule was observed (at a cms energy of about 80 MeV above the  $\phi$  production threshold). Further experimental investigations of the reactions  $pp \rightarrow pp\phi$  and  $pp \rightarrow pp\omega$ , as well as  $pn \rightarrow d\phi$  and  $pn \rightarrow d\omega$ , closer to their thresholds, are planned for the near future at the COSY facility in Jülich [11,12].

Recently we have developed a model for the reactions  $pp \rightarrow pp\omega$  and  $pp \rightarrow pp\phi$  within the conventional meson-exchange picture [13,14]. In this model meson production is described by the two mechanisms depicted in Fig. 1, namely the nucleonic current and the  $\pi\rho v$  ( $v = \omega, \phi$ ) meson exchange current. Those two processes were identified as providing the dominant contributions to these vector-meson production reactions. We employed this model for a combined analysis of close-to-threshold  $\phi$  and  $\omega$  production data with special emphasis on the apparent OZI rule violation reported by the DISTO collaboration. It turned out that the data do not require a large  $NN\phi$  coupling constant. Indeed, the range of values for  $g_{NN\phi}$  extracted from this analysis was found to be compatible with the OZI value [14] - which might be interpreted as an indication that there is no need for introducing an  $\bar{s}s$  component into the nucleon in order to describe those data. On the other hand, it was necessary to introduce a violation of the OZI rule at the  $\pi\rho\phi$  vertex in the meson-exchange current - which, in turn, provided the enhancement of the  $\phi$  production cross section over the OZI estimation as seen in the DISTO data.

In the present paper we apply this model to the reactions  $pn \rightarrow d\omega$  and  $pn \rightarrow d\phi$ . First of all, it is desirable to have quantitative results for those reaction channels. In this context we would like to emphasize that all our model parameters have already been fixed in the previous study [14], where they were constrained by requiring a consistent description of the reactions  $pp \rightarrow pp\omega$  and  $pp \rightarrow pp\phi$ . Therefore we are able to provide genuine predictions for observables for  $pn \rightarrow d\omega$  and  $pn \rightarrow d\phi$ . Such predictions should be very useful for corresponding measurements that are planned at the COSY facility in Jülich. Furthermore they can be used for testing the reliability of our model when data become available in the future.

Secondly, in our previous studies [13,14] we found that the angular distribution of the produced vector mesons is very sensitive to the production mechanisms. We showed that this angular distribution enables us to determine both the relative importance of the basic

reaction mechanisms (cf. Fig. 1) and their absolute magnitudes. In fact, it was this special feature that enabled us to extract the  $\phi NN$  coupling constant from the analysis in Ref. [14]. Thus it is interesting to see whether a similar signature is also present in the reactions  $pn \rightarrow d\omega$  and  $pn \rightarrow d\phi$  and, specifically, whether these reactions are even better suited for discriminating between the different production mechanisms.

Finally, in the aftermath of the LEAR experiments, Ellis et al. [15] proposed a qualitative model in which it is assumed that the nucleon contains, besides  $u$  and  $d$  quarks, an intrinsic  $\bar{s}s$  component. In this model  $\phi$  production proceeds via a “shake-out” or a “rearrangement” of the  $s$  and  $\bar{s}$  quarks in the nucleon. Assuming, furthermore, that the  $\bar{s}s$  component in the nucleon is polarized introduces selection rules for the various  $\phi$  production channels and allows a qualitative interpretation of the state dependence shown by the  $\bar{p}p$  annihilation data. Recently this picture has also been used for some qualitative estimates for the  $\phi$  production in  $NN$  collisions [16]. It is interesting to explore whether the predictions of our conventional model differ from the results that would follow from the picture of Ellis et al.

The paper is structured in the following way: In Section II we give a review of our relativistic meson-exchange model for vector-meson production. In Section III we present and discuss our results for the reactions  $pn \rightarrow d\omega$  and  $pn \rightarrow d\phi$ . The paper concludes with a short summary.

## II. THE MODEL

We study the reaction  $pn \rightarrow dv$  ( $v = \omega, \phi$ ) in a DWBA approach [13,14]. The transition amplitude is given by

$$M^\mu = \langle \psi_d | J^\mu | \phi_i \rangle , \quad (1)$$

where  $\psi_d$  is the deuteron wave function and  $\phi_i$  is the four-component unperturbed  $NN$  wave function in the initial state. We take the deuteron wave function of the model Bonn B as defined in Table A.1 of Ref. [17]. (Note that this model has been also used to generate the  $pp$  final state interaction in our previous study [13,14] of the  $pp \rightarrow ppv$  reaction.)  $J^\mu$  is the current describing the vector-meson production process. In our model  $J^\mu$  is given by the sum of the nucleonic and  $\nu\rho\pi$  meson-exchange currents,  $J^\mu = J_{nuc}^\mu + J_{mec}^\mu$ , as illustrated diagrammatically in Fig. 1. In principle there are, of course, many more meson-exchange currents that could contribute. Their relevance was thoroughly investigated in [14] and it was found that all other exchange currents yield contributions that are much smaller than those of the  $\nu\rho\pi$  meson-exchange current.

Explicitly, the nucleonic current is defined as

$$J_{nuc}^\mu = \sum_{j=1,2} \left( \Gamma_j^\mu i S_j U + U i S_j \Gamma_j^\mu \right) , \quad (2)$$

with  $\Gamma_j^\mu$  denoting the  $NNv$  vertex and  $S_j$  the nucleon (Feynman) propagator for nucleon  $j$ . The summation runs over the two interacting nucleons, 1 and 2.  $U$  stands for the meson-exchange  $NN$  potential. It is, in principle, identical to the driving potential [17] used in the calculation of the deuteron wave function  $\psi_d$  in Eq. (1), except that here meson retardation effects are retained following the Feynman prescription. Eq. (2) is illustrated in Fig. 1a.

The structure of the  $NNv$  vertex,  $\Gamma^\mu$  (the subscript  $j = 1, 2$  is omitted), required in Eq. (2) for the production is obtained from the Lagrangian density

$$\mathcal{L}(x) = -\bar{\Psi}(x) \left( g_{NNv} [\gamma_\mu - \frac{\kappa_v}{2m_N} \sigma_{\mu\nu} \partial^\nu] V^\mu(x) \right) \Psi(x) , \quad (3)$$

where  $\Psi(x)$  and  $V^\mu(x)$  stand for the nucleon and vector-meson fields, respectively.  $g_{NNv}$  denotes the vector coupling constant and  $\kappa_v \equiv f_{NNv}/g_{NNv}$ , with  $f_{NNv}$  the tensor coupling constant.  $m_N$  denotes the nucleon mass.

As in most meson-exchange models of interactions, each hadronic vertex is furnished with a form factor in order to account for, among other things, the composite nature of the hadrons involved. In this spirit the  $NNv$  vertex obtained from the above Lagrangian is multiplied by a form factor. The theoretical understanding of this form factor is beyond the scope of the present paper; we assume it to be of the form

$$F_N(l^2) = \frac{\Lambda_N^4}{\Lambda_N^4 + (l^2 - m_N^2)^2} , \quad (4)$$

where  $l^2$  denotes the four-momentum squared of either the incoming or outgoing off-shell nucleon. It is normalized to unity when the nucleon is on its mass-shell,  $l^2 = m_N^2$ .

The  $v\rho\pi$  vertex required for constructing the meson-exchange current,  $J_{mec}^\mu$  (Fig. 1b), is derived from the Lagrangian density

$$\mathcal{L}_{v\rho\pi}(x) = \frac{g_{v\rho\pi}}{\sqrt{m_v m_\rho}} \varepsilon_{\alpha\beta\nu\mu} \partial^\alpha \bar{\rho}^\beta(x) \cdot \partial^\nu \vec{\pi}(x) V^\mu(x) , \quad (5)$$

where  $\varepsilon_{\alpha\beta\nu\mu}$  denotes the Levi-Civita antisymmetric tensor with  $\varepsilon_{0123} = -1$ . The  $v\rho\pi$  vertex obtained from the above Lagrangian is multiplied by a form factor which is taken to be of the form

$$F_{v\rho\pi}(q_\pi^2, q_\rho^2) = \left( \frac{\Lambda_M^2 - m_\pi^2}{\Lambda_M^2 - q_\pi^2} \right) \left( \frac{\Lambda_M^2 - x m_\rho^2}{\Lambda_M^2 - q_\rho^2} \right) . \quad (6)$$

It is normalized to unity at  $q_\pi^2 = m_\pi^2$  and  $q_\rho^2 = x m_\rho^2$ . The parameter  $x$  ( $= 0$  or  $1$ ) is introduced in order to allow for different normalization points in order to take into account that the values of the  $v\rho\pi$  coupling constants that we employ are extracted at different kinematics [14].  $g_{\phi\rho\pi}$  is determined at  $q_\rho^2 = m_\rho^2$  and  $q_\pi^2 = m_\pi^2$ , whereas  $g_{\omega\rho\pi}$  is extracted at  $q_\rho^2 = 0$  and  $q_\pi^2 = m_\pi^2$ . Accordingly, we use the normalization  $x = 1$  for the form factor at the former vertex and  $x = 0$  for the latter.

The meson-exchange current is then given by

$$J_{mec}^\mu = [\Gamma_{NN\rho}^\alpha(q_\rho)]_1 i D_{\alpha\beta}(q_\rho) \Gamma_{v\rho\pi}^{\beta\mu}(q_\rho, q_\pi, k_\omega) i \Delta(q_\pi) [\Gamma_{NN\pi}(q_\pi)]_2 + (1 \leftrightarrow 2) , \quad (7)$$

where  $D_{\alpha\beta}(q_\rho)$  and  $\Delta(q_\pi)$  stand for the  $\rho$ - and  $\pi$ -meson (Feynman) propagators, respectively. The vertices  $\Gamma$  involved are self-explanatory. Both the  $NN\rho$  and  $NN\pi$  vertices,  $\Gamma_{NN\rho}^\alpha$  and  $\Gamma_{NN\pi}$ , are taken consistently with the  $NN$  potential used to generate the deuteron wave function in Eq. (1).

Our model described above contains five parameters to be fixed for a given vector-meson produced: two for the mesonic current (the coupling constant  $g_{v\rho\pi}$  and the cutoff parameter  $\Lambda_M$ ) and three for the nucleonic current (the coupling constants  $g_{NNv}$  and  $f_{NNv}$ , and the cutoff parameter  $\Lambda_N$ ).

The coupling constant  $g_{\phi\rho\pi}$  was extracted from the measured decay width ( $\phi \rightarrow \rho + \pi$ ) and  $g_{\phi\rho\pi}$  from the radiative decay width ( $\omega \rightarrow \gamma + \pi$ ) assuming vector meson dominance. All other parameters were fixed in a combined analysis of all available near-threshold data on  $\phi$ - and  $\omega$ -meson production in  $pp$  collisions [14]. Besides using the data from both reactions, we also assumed relations between corresponding parameters in the production amplitudes. Specifically, we assumed that the form factors at the  $\phi\rho\pi$  and  $\omega\rho\pi$  vertices are the same. Likewise, we assumed that the form factor at the meson production vertices in the nucleonic current are the same. The  $NN\omega$  coupling constant is fixed to the SU(3) value,  $g_{NN\omega} = 9$ , based on  $g_{NN\rho}$  of Ref. [18]. Furthermore we assumed that  $\kappa_\phi = \kappa_\omega \equiv \kappa$ , as also suggested by SU(3) symmetry, with  $-0.5 \leq \kappa \leq 0.5$ .

Details of our strategy for fixing the model parameters are outlined in Ref. [14]. Here we only want to mention that the lack of a more complete set of data prevented us from achieving a unique solution. Rather, we arrived at four different model solutions that all provide a comparably good description of the data but differ in the value of the nucleon cutoff mass  $\Lambda_N$ , the value of  $g_{NN\phi}$  and the value of  $\kappa$ , cf. Table I. We shall employ all these model solutions in the present investigation.

Finally, we want to mention that the initial state interaction (ISI) is not taken into account explicitly in our model. Rather, its effect is accounted for effectively via an appropriate adjustment of the (phenomenological) form factors at the hadronic vertices, cf. the corresponding statements in Ref. [14]. Admittedly, this procedure leads to a certain degree of uncertainty of our predictions because the ISI in the reactions  $pn \rightarrow dv$  and  $pp \rightarrow ppv$ , respectively, is governed by different partial waves (different isospin states). On the other hand, we don't have at present any better and more solid alternative for dealing with the ISI interaction. There are no  $NN$  interaction models in the literature that are still valid in the energy range relevant for  $\omega$  and  $\phi$  production for an explicit treatment of ISI effects. Furthermore, the qualitative prescription proposed in Ref. [19], based on phase shifts and inelasticity parameters, can't be used either because there is no reliable phase shift analysis beyond 1.3 GeV for the isospin  $T = 0$  channel [20] that we need here.

### III. RESULTS AND DISCUSSION

The data that were used in Ref. [14] to fix the free parameters of our model consisted of some near-threshold total cross sections for the reaction  $pp \rightarrow pp\omega$  [21] and of the total cross section, as well as the angular distribution of the  $\phi$  at  $T_{lab} = 2.85$  GeV for the reaction  $pp \rightarrow pp\phi$  [10]. Naturally, the more selective experimental information available for the latter reaction (angular distributions) put also a stronger constraint on the model parameters and, as a consequence, the predictions for  $pn \rightarrow d\phi$  for the four parameter sets in Table I don't differ much. As a matter of fact, the general features of the results are practically identical and therefore we show only the predictions for one of the sets (set 1 of Table I) in Fig. 2. Values for the total cross section at a few excess energies  $Q$  are, however, compiled in

Table II for all parameter sets. It is evident from Fig. 2 that the reaction  $pn \rightarrow d\phi$  is strongly dominated by the meson exchange current. The relative magnitude of the contribution from the nucleonic current is even smaller than in case of  $pp \rightarrow pp\phi$ ; it was about 18 % there, here it is a mere 3 %. The stronger suppression of the nucleonic current in the reaction  $pn \rightarrow d\phi$  is due to the fact that the meson exchange current is weighted by a larger isospin coefficient (-3 for  $pn \rightarrow d\phi$  as compared to +1 in the case  $pp \rightarrow pp\phi$ ). The nucleonic current, however, has contributions from the exchange of iso-scalar as well as iso-vector mesons. Consequently, only the latter are multiplied by a larger isospin coefficient. Furthermore, since the isospin factor changes sign, there are now also cancellations between the meson exchanges that contribute to the nucleonic current. As in the case of  $pp \rightarrow pp\phi$ , there is a destructive interference between the nucleonic current and the meson exchange current which, however, is now much less pronounced. Nonetheless, the predicted angular distributions of the emitted  $\phi$  meson, which are fairly flat, show some downward bending at very forward and backward angles as a consequence of this destructive interference between the two production mechanisms, cf. Fig. 3. For higher energies (Fig. 3,  $Q = 100\text{MeV}$ ) the suppression of the angular distribution at forward and backward angles becomes more pronounced and it should be possible to verify experimentally whether the angular distribution does indeed have such a structure. In general there is not much difference between the angular distributions resulting from the four parameter sets, except that those with  $\kappa = 0.5$  yield a total cross section which is about 20 % larger, cf. also Table II.

Predictions of total cross sections for the reaction  $pn \rightarrow d\omega$  for the four parameter sets are shown in Fig. 4. Also here we observe that the meson exchange current is the dominant production mechanism. Its relative importance is likewise increased compared to  $pp \rightarrow pp\omega$ . Indeed, now the meson exchange current dominates for all four parameter sets, whereas in the reaction  $pp \rightarrow pp\omega$  it is the nucleonic current that provides the dominant contribution for the parameter sets 2 and 4. Still, in all cases, the nucleonic current is large enough to introduce sizable interference effects. Consequently, we obtain a much stronger variation of the predicted total cross sections for  $pn \rightarrow d\omega$  than for  $pn \rightarrow d\phi$ . The results vary by a factor of roughly 3, as can be seen from Fig. 4 and also from Table II. Note that there are particularly strong interference effects in case of parameter set 2 (Fig. 4b), where the resulting total cross section is significantly smaller than the individual contributions. As we shall discuss later, the stronger variations in the  $\omega$  production cross section have also consequences for the cross section ratio  $R_{\phi/\omega} \equiv \sigma_{pn \rightarrow d\phi} / \sigma_{pn \rightarrow d\omega}$  relevant for the comparison with the corresponding ratio that follows from the OZI rule.

We observe that for  $Q \leq 20$  MeV, effects from the finite width of the  $\omega$  meson become important. These effects are included in our calculation by folding the calculated cross section with the Breit-Wigner mass distribution of the  $\omega$  meson and can be seen in Fig. 4.

Predictions for the angular distribution of the  $\omega$  meson are displayed in Fig. 5. Naturally, here we see also larger variations between the predictions for the different parameter sets. But, since the meson exchange current is the dominant production mechanism for all sets, all the angular distributions show qualitatively a similar structure, i.e. they are rather flat at the lower energy ( $Q = 30$  MeV) and exhibit a more-or-less strong downward bending at forward and backward angles at the higher energy ( $Q = 100$  MeV). We would like to emphasize, however, that this behavior differs from the one in the reaction  $pp \rightarrow pp\omega$ . In the latter reaction a clear enhancement of the angular distribution in forward and backward direction

was seen in the DISTO experiment [10] (at  $T_{lab} = 2.85$  MeV), and such an enhancement for the reaction  $pp \rightarrow pp\omega$  is also predicted by our model (parameter sets 2 and 4) - even for energies closer to the  $\omega$  production threshold.

As a general feature, let us also mention that the cross sections for the reactions  $pn \rightarrow dv$  are significantly larger than the ones for  $pp \rightarrow ppv$  near threshold. Apart from the isospin factors involved, such a behavior can be understood in terms of phase space arguments (the two body phase space opens up more rapidly close to threshold) and is well-known from other meson production reactions (see, e.g., Refs. [22,23]).

We now turn our attention to the cross section ratio  $R_{\phi/\omega} = \sigma_{pn \rightarrow d\phi} / \sigma_{pn \rightarrow d\omega}$  for a comparison with the prediction that follows from the naive application of the OZI rule [4]. The adjective “naive” refers to the fact that the cross section ratio is simply equated to the square of the ratio of the relevant coupling constants at the  $\phi$  and  $\omega$  production vertices. The OZI rule plus SU(3) imply that these coupling constants are proportional to  $\sin \alpha_v$  and  $\cos \alpha_v$ , respectively, where  $\alpha_v$  stands for the deviation of the  $\phi$ - $\omega$  mixing angle from its ideal mixing value of  $\theta_{(ideal)} = 35.3^\circ$ . Thus the OZI estimate for the cross section ratio is simply given by  $R_{\phi/\omega} = \tan^2 \alpha_v$  [4]. With  $\alpha_v = 3.7^\circ$  as extracted from the quadratic mass formula, this yields a value of  $R_{\phi/\omega} = 4.2 \times 10^{-3}$ .

Our results for  $R_{\phi/\omega}$  are presented in Fig. 6. The cross sections are evaluated at the same excess energy in order to minimize effects from differences in the phase space. We see that the largest values are predicted for excess energies close to threshold. E.g., at  $Q \approx 10$  MeV we get values between  $32 \times 10^{-3}$  (set 2) and  $9 \times 10^{-3}$  (set 3). Thus, compared to the ratio that follows from the naive OZI rule,  $R_{\phi/\omega} = 4.2 \times 10^{-3}$ , our models yield a moderate deviation of at most a factor of 8. At higher energies,  $Q = 80 \sim 100$  MeV, the enhancement over the OZI estimate decreases to a factor of around 3 or so.

So, what is the origin of this enhancement over the OZI estimate as predicted by our model? As already mentioned in the Introduction, our model involves an explicit violation of the OZI rule at the  $\pi\rho\phi$  vertex in the meson exchange current. As discussed in detail in Ref. [14], it had to be introduced in order to achieve a simultaneous and consistent description within our model of the available data on the reactions  $pp \rightarrow pp\omega$  and  $pp \rightarrow pp\phi$ , particularly of the energy dependence of the total  $\omega$  production cross section and the angular distribution of the  $\phi$  meson. This explicit OZI violation, in terms of the  $\pi\rho\phi$  and  $\pi\rho\omega$  coupling constants used, suggests an enhancement of around 3 in the cross section ratio. With regard to the nucleonic current, the employed  $NN\omega$  and  $NN\phi$  coupling constants lead to results that exceed the OZI value only in one case, namely for parameter set 3, cf. Table I. The corresponding enhancement factor for the cross section ratio amounts to around 2.

It is evident from Fig. 6 that the cross section ratios resulting from the full model calculation differ significantly from those values implied by the employed coupling constants. Obviously dynamical effects such as interferences, energy dependence of the production amplitudes, etc. play a rather important role here. For example, parameter set 3 - which is the only model where the  $NN\phi$  coupling exceeds the OZI value - yields the smallest enhancement over the naive OZI estimate among all models considered, cf. the dash-dotted curve in Fig. 6. Furthermore, the particularly large enhancement over the OZI estimate found for parameter set 2 (especially at small excess energies) is, in fact, due to a suppression of the  $\omega$  production cross section (resulting from strong interference effects as pointed out above) and not caused by an enhancement in the  $\phi$  production, cf. Table II. Apparently fairly

large deviations from the naive OZI prediction can be generated by dynamical effects within the conventional picture: i.e., without introducing any "exotic" mechanisms. Consequently, one should be very cautious in drawing direct conclusions on the strangeness content in the nucleon from such cross section ratios. The behavior of the cross section ratio as the excess energy approaches zero is due to the finite width of the  $\omega$ -meson which prevents the  $\omega$ -meson production cross section from decreasing rapidly as it does in the case of  $\phi$ -meson, cf. Figs. 2,4.

Evidently, the enhancement of a factor of 3 or so over the OZI estimate at higher excess energies in Fig. 6 is much smaller than the enhancement over the OZI estimate of about a factor 10 found for  $\sigma_{pp \rightarrow pp\phi}/\sigma_{pp \rightarrow pp\omega}$  by the DISTO collaboration [10] at an excess energy  $Q \approx 80$  MeV of the  $\phi$ . However it is important to realize that their measurement was done at a fixed incident beam energy ( $T_{lab} = 2.85$  GeV); therefore the corresponding excess energy of the produced  $\omega$  is already 319 MeV. Although corrections for the differences in the available phase space were obviously applied when extracting the above result, there are other effects that influence the ratio such as the energy dependence of the production amplitude, the onset of higher partial waves, etc., which one cannot correct for easily. Therefore it is possible that the actual deviation from the naive OZI rule in the reactions  $pp \rightarrow ppv$  is also smaller. Indeed our results for  $\sigma_{pp \rightarrow pp\phi}/\sigma_{pp \rightarrow pp\omega}$ , shown in Fig. 7, support this conjecture. We see here that the results are very similar to the ones for  $\sigma_{pn \rightarrow d\phi}/\sigma_{pn \rightarrow d\omega}$ . Specifically, at the excess energy of  $Q = 80$  MeV the enhancement over the OZI estimate is also only around a factor 3. Thus it would be interesting to perform a measurement of the ratio  $\sigma_{pp \rightarrow pp\phi}/\sigma_{pp \rightarrow pp\omega}$  at the same (or at least similar) excess energies.

Finally, let us comment on a recent work by Ellis et al. [16]. This work builds upon the assumption that the nucleon wave function contains an admixture of negatively polarized  $\bar{s}s$  quark pairs and allows one to deduce some qualitative predictions for the state dependence of  $\phi$  production in  $\bar{N}N$ , but also in  $NN$  collisions too. Specifically, this picture has been used to explain the observed differences in the branching ratios for  $\bar{p}p \rightarrow \phi\pi^0$  at rest - which is rather large and OZI violating when the initial  $\bar{p}p$  system is in a  $^3S_1$  state, but small and consistent with the OZI rule for the  $^1P_1$  initial state. With regard to  $\phi$  production in  $NN$  collisions, it is argued that  $\phi$  production should be likewise much larger from initial spin-triplet states [16]. Specifically, this means that the  $\phi$  production cross section in the  $pp$  induced reaction is expected to be enhanced over the OZI rule because, close to threshold, it will proceed predominantly via the transition  $^3P_1 \rightarrow ^1S_0s$ . (We use here the standard nomenclature for labeling the partial waves of the  $NN$  states and the angular orbital momentum of the  $\phi$  relative to the final  $NN$  system.) On the other hand, for  $pn$  induced reactions like  $pn \rightarrow d\phi$ , the production amplitude is given by the transition  $^1P_1 \rightarrow ^3S_1s$  and should therefore be OZI suppressed. In contrast, our dynamical model predicts cross section ratios of comparable magnitude for the  $pp \rightarrow ppv$  and  $pn \rightarrow dv$  reactions, as can be seen from a comparison of Figs. 6 and 7. Clearly, experimental information on these ratios would be very useful.

#### IV. SUMMARY

We have investigated the reactions  $pn \rightarrow d\phi$  and  $pn \rightarrow d\omega$  near threshold in a relativistic meson-exchange model. The elementary vector-meson production mechanism is provided by



the nucleonic and the  $\phi\rho\pi$  (and  $\omega\rho\pi$ , respectively) meson-exchange currents. The presented results for total cross sections and for the angular distributions of the vector mesons are true predictions. All model parameters have been taken from a previous study of the reactions  $pp \rightarrow pp\phi$  and  $pp \rightarrow pp\omega$  [14].

A clear consequence of the model is that the reaction  $pn \rightarrow d\phi$  is almost completely dominated by the meson exchange current. The contributions from the nucleonic current, which were found to be already small for  $pp \rightarrow pp\phi$ , are now even less significant - especially for the total cross section. The angular distribution of the  $\phi$  meson, however, still reflects some influence of the nucleonic current through interference effects. It is predicted to be rather flat for excess energies  $Q \lesssim 30$  MeV but to show an increasing suppression of very forward and backward angles for higher energies.

In case of the reaction  $pn \rightarrow d\omega$  the contributions from the nucleonic current are somewhat larger. Thus, stronger interference effects between this current and the meson-exchange current are possible. As a consequence, the predictions for  $pn \rightarrow d\omega$  based on the four parameter sets of Ref. [14] differ much more than those for  $pn \rightarrow d\phi$ , showing variations by up to a factor 3 in the total cross sections. This also implies greater variations in the cross section ratio  $\sigma_{pn \rightarrow d\phi} / \sigma_{pn \rightarrow d\omega}$ , for which our model yields values that exceed the estimate based on the naive OZI rule by factors of up to 8.

#### ACKNOWLEDGMENTS

We would like to thank J. Durso for a careful reading of the manuscript.

## REFERENCES

- [1] J.F. Donoghue and C.R. Nappi, Phys. Lett. **B168**, 105 (1986); J. Gasser, H. Leutwyler, and M.E. Sainio, Phys. Lett. **B253**, 252 (1991).
- [2] J. Ashman et al., Phys. Lett. **B206**, 364 (1988).
- [3] S. Okubo, Phys. Lett. **5**, 165 (1963); G. Zweig, CERN Report No. TH412, 1964; J. Iizuka, Prog. Theor. Phys. Suppl. **37 & 38**, 21 (1966).
- [4] H.J. Lipkin, Phys. Lett. **60B**, 371 (1976).
- [5] J. Reifenröther et al., Phys. Lett. **B267**, 299 (1991).
- [6] C. Amsler et al., Z. Phys. **C58**, 175 (1993); Z. Weidenauer et al., Z. Phys. **C59**, 387 (1993); C. Amsler et al., Phys. Lett. **B346**, 363 (1995).
- [7] V.G. Ableev et al., Phys. Lett. **B334**, 237 (1994); V.G. Ableev et al., Nucl. Phys. **A585**, 577 (1995); V.G. Ableev et al., Nucl. Phys. **A594**, 375 (1995); A. Bertin et al., Phys. Lett. **B388**, 450 (1996).
- [8] R. Wurzinger et al., Phys. Lett. **B374**, 283 (1996).
- [9] L. Bertolotto et al., Phys. Lett. **B345**, 325 (1995); C. Evangelista et al., Phys. Rev. **D 57**, 5370 (1998).
- [10] F. Balestra et al., Phys. Rev. Lett. **81**, 4572 (1998).
- [11] M. Büscher et al., COSY Proposal no. 75 (1998),  
<http://ikpd15.ikp.kfa-juelich.de:8085/doc/Proposals.html>
- [12] COSY 11 collaboration, COSY Proposal no. 78 (1998),  
[http://ikpe1101.ikp.kfa-juelich.de/cosy-11/pub/List\\_of\\_Publications.html#props](http://ikpe1101.ikp.kfa-juelich.de/cosy-11/pub/List_of_Publications.html#props)
- [13] K. Nakayama, A. Szczurek, C. Hanhart, J. Haidenbauer, and J. Speth Phys. Rev. **C57**, 1580 (1998).
- [14] K. Nakayama, J.W. Durso, J. Haidenbauer, C. Hanhart, and J. Speth Phys. Rev. **C60**, 055209 (1999).
- [15] J. Ellis, M. Karliner, D.E. Kharzeev, and M.G. Sapozhnikov, Phys. Lett. **B353**, 319 (1995).
- [16] J. Ellis, M. Karliner, D.E. Kharzeev, and M.G. Sapozhnikov, [hep-ph/9909235](http://arxiv.org/abs/hep-ph/9909235).
- [17] R. Machleidt, Adv. Nucl. Phys. **19**, 189 (1989).
- [18] G. Höhler and E. Pietarinen, Nucl. Phys. **B95**, 210 (1975).
- [19] C. Hanhart and K. Nakayama, Phys. Lett. **B 454**, 176 (1999).
- [20] R.A. Arndt, I.I. Strakovsky, and R.L. Workman, [nucl-th/0004039](http://arxiv.org/abs/nuc1-th/0004039).
- [21] F. Hibou et al., Phys. Rev. Lett. **83**, 492 (1999).
- [22] H.O. Meyer, Annu. Rev. Nucl. Part. Sci. **47**, 235 (1997).
- [23] H. Calén et al., Phys. Rev. C **58**, 2667 (1998).

## TABLES

TABLE I. Parameters of the four different models employed in the present study. The values  $g_{\phi\rho\pi} = -1.64$ ,  $g_{\omega\rho\pi} = 10$ ,  $g_{NN\omega} = 9$ , and  $\Lambda_M = 1450$  MeV are used for all four sets.  $\kappa \equiv \kappa_v = f_{NNv}/g_{NNv}$  with  $v = \phi, \omega$ .

Set	1	2	3	4
$\kappa$	-0.5	-0.5	+0.5	+0.5
$\Lambda_N$	1170	1411	1312	1545
$g_{NN\phi}$	-0.45	-0.19	-0.90	-0.40

TABLE II. Total cross sections for the reactions  $pn \rightarrow d\omega$  and  $pn \rightarrow d\phi$  resulting from the model parameter sets 1 - 4 at selected excess energies  $Q$ .

	$pn \rightarrow d\phi$ $\sigma_{tot}$ (nb)				$pn \rightarrow d\omega$ $\sigma_{tot}$ ( $\mu\text{b}$ )			
Set	1	2	3	4	1	2	3	4
$Q = 30$ MeV	219.9	216.4	265.8	253.1	19.2	9.4	31.1	26.9
$Q = 60$ MeV	283.8	279.6	341.3	323.8	27.2	17.7	41.8	38.9
$Q = 100$ MeV	322.4	318.2	385.4	364.2	34.1	26.9	49.9	50.2

## FIGURES

FIG. 1.  $\phi$  and  $\omega$ -meson production currents,  $J^\mu$ , included in the present study: (a) nucleonic current, (b)  $\nu\rho\pi$  meson exchange current.  $M = \pi, \eta, \rho, \omega, \sigma, a_0$ .

FIG. 2. Total cross section for the reaction  $pn \rightarrow d\phi$  as predicted by the model set 1 of Table I as a function of excess energy  $Q$ . The solid line is the result of the full model. The dashed (dash-dotted) curves show the contributions of the nucleonic current (meson exchange current) alone.

FIG. 3. Angular distribution in the center-of-mass system of the produced  $\phi$ -meson in the reaction  $pn \rightarrow d\phi$  at the excess energies  $Q = 30$  MeV (left panel) and 100 MeV (right panel). The dashed, solid, dashed-dotted and dotted curves are the results for the model parameter sets 1, 2, 3, and 4.

FIG. 4. Same as Fig. 2 for the reaction  $pn \rightarrow d\omega$  as predicted by the model sets 1 (a), 2 (b), 3 (c), and 4 (d) of Table I. The dotted curves correspond to the results with the sharp mass of  $728.6\text{MeV}$  for the  $\omega$ -meson.

FIG. 5. Same as Fig. 3 for the reaction  $pn \rightarrow d\omega$ .

FIG. 6. Ratio of the total cross sections  $\sigma_{pn \rightarrow d\phi}/\sigma_{pn \rightarrow d\omega}$  as a function of excess energy  $Q$ . The dashed, solid, dashed-dotted and dotted curves are the results for the model parameter sets 1, 2, 3, and 4. The horizontal solid line indicates the value predicted by the naive OZI rule.

FIG. 7. Same as Fig. 6 for the ratio  $\sigma_{pp \rightarrow pp\phi}/\sigma_{pp \rightarrow pp\omega}$ .

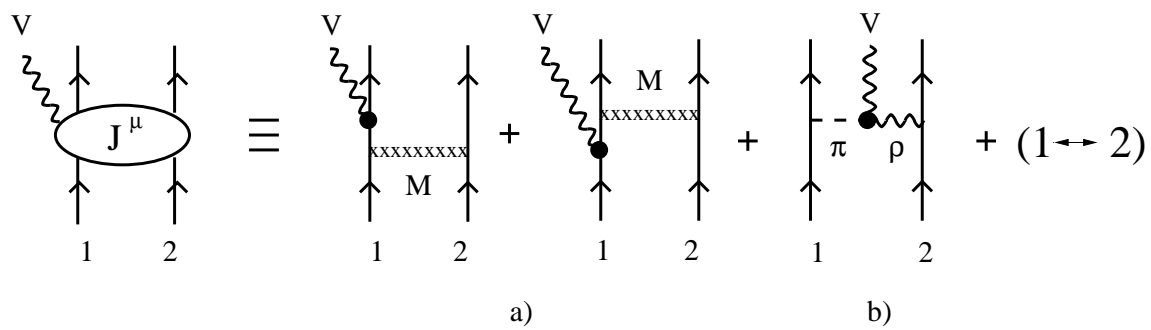


Fig. 1

Fig. 2

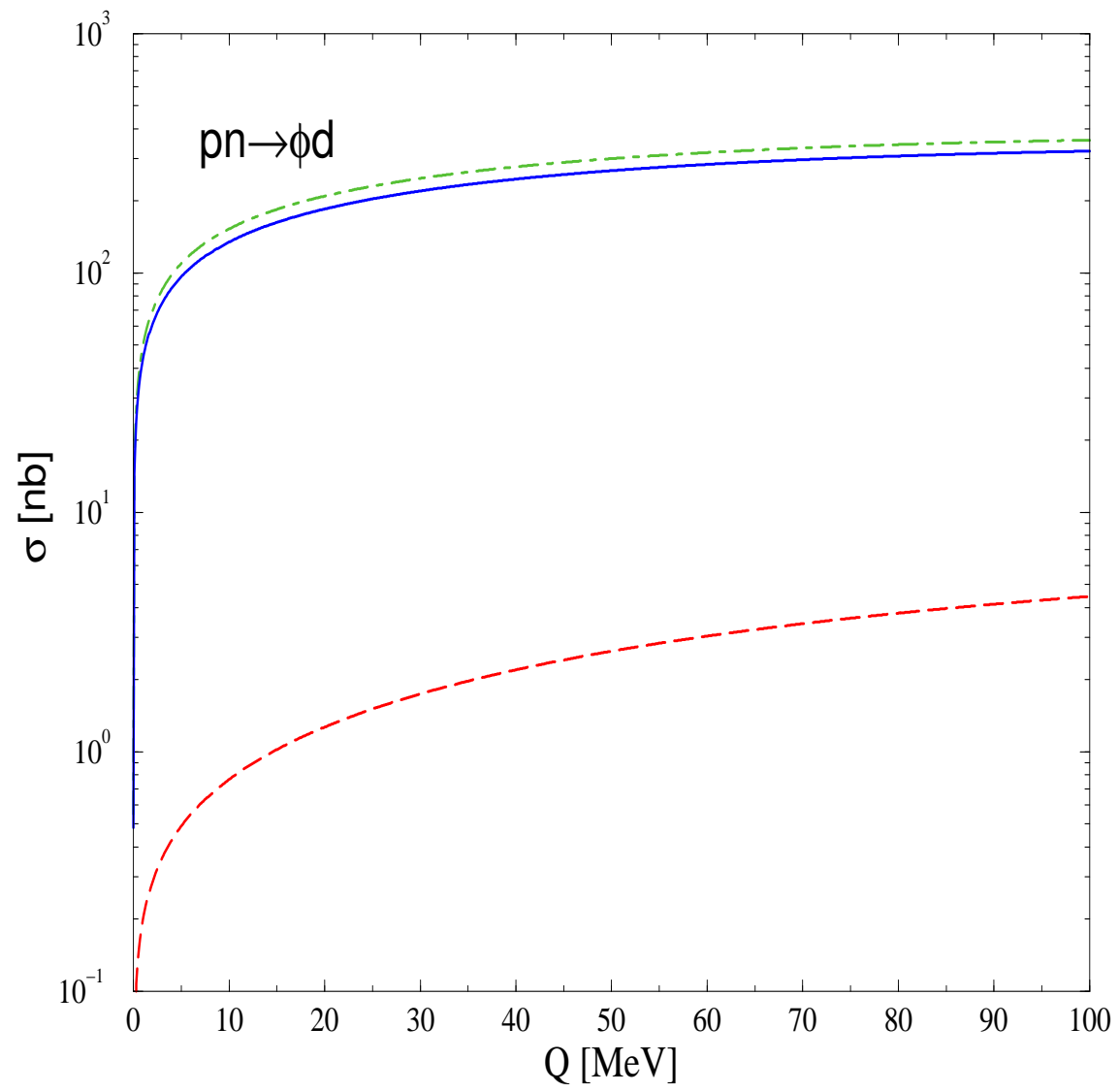


Fig. 3

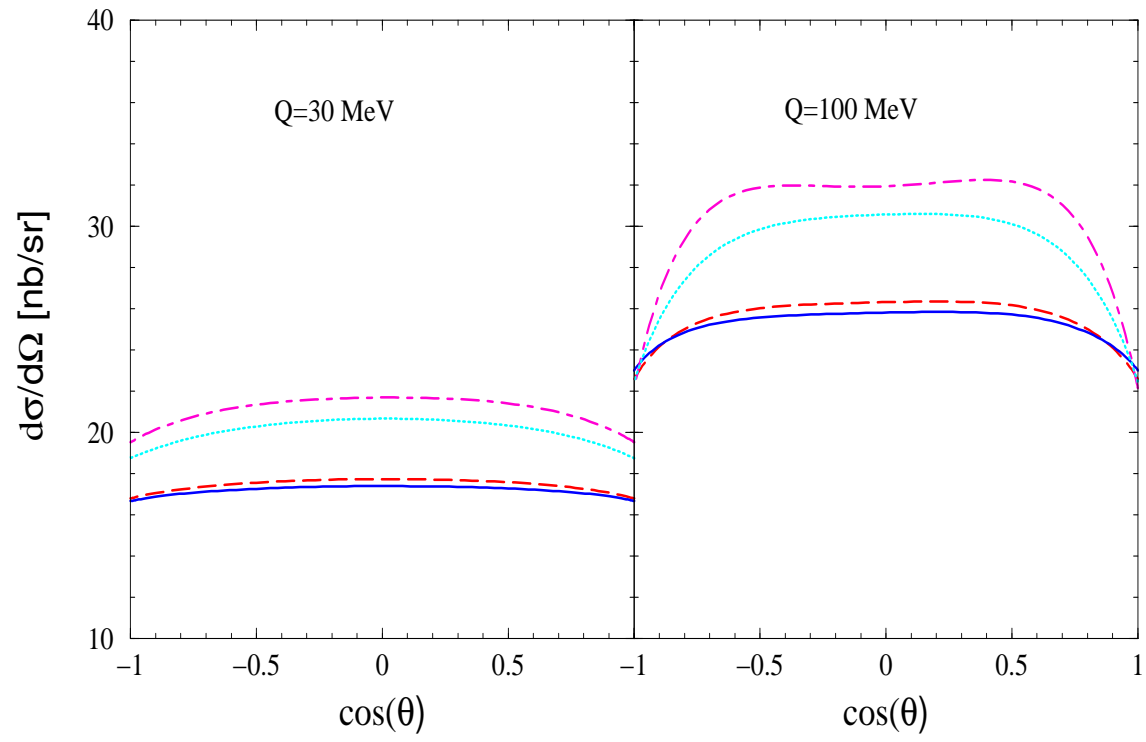


Fig. 4

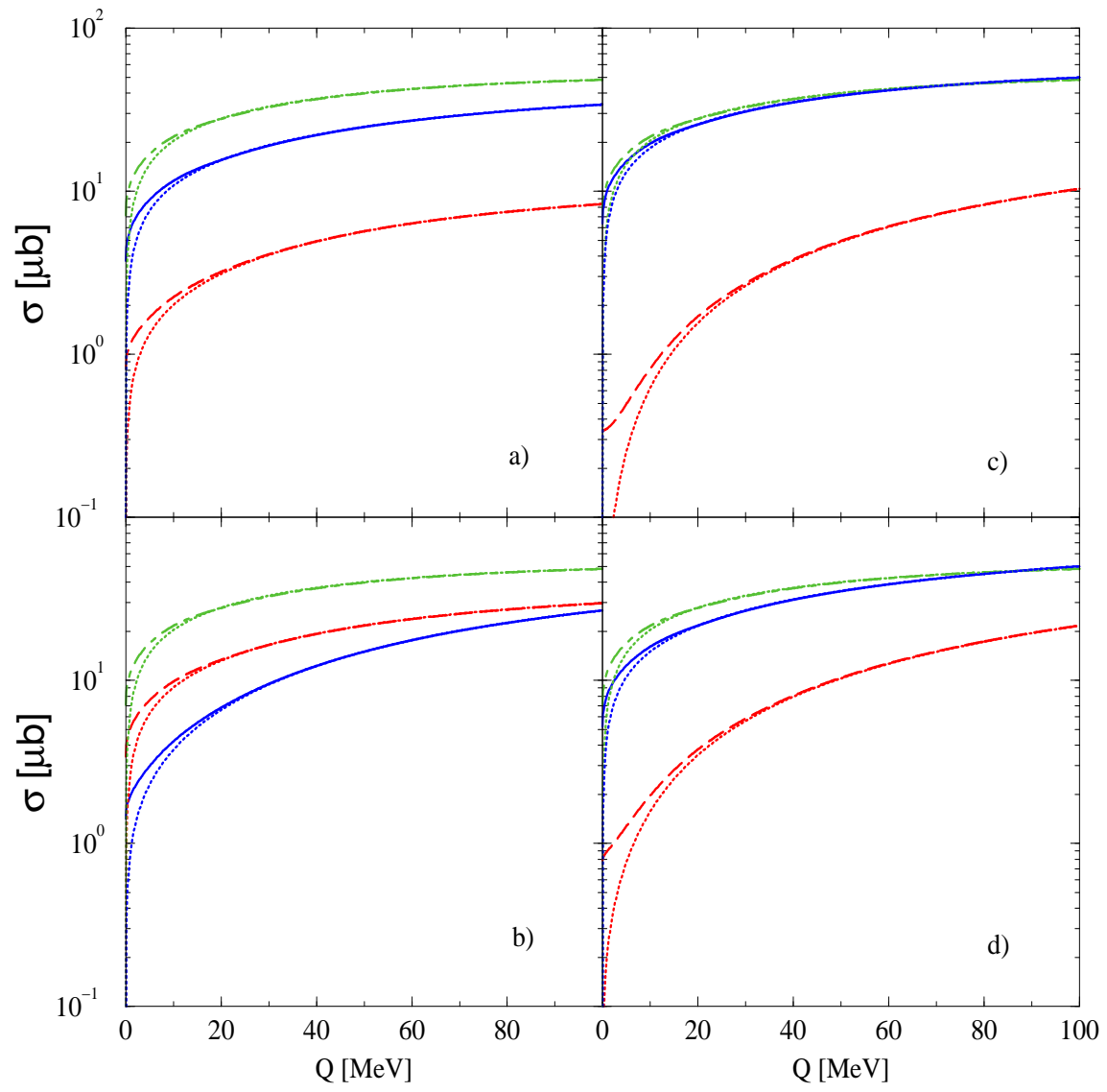




Fig. 5

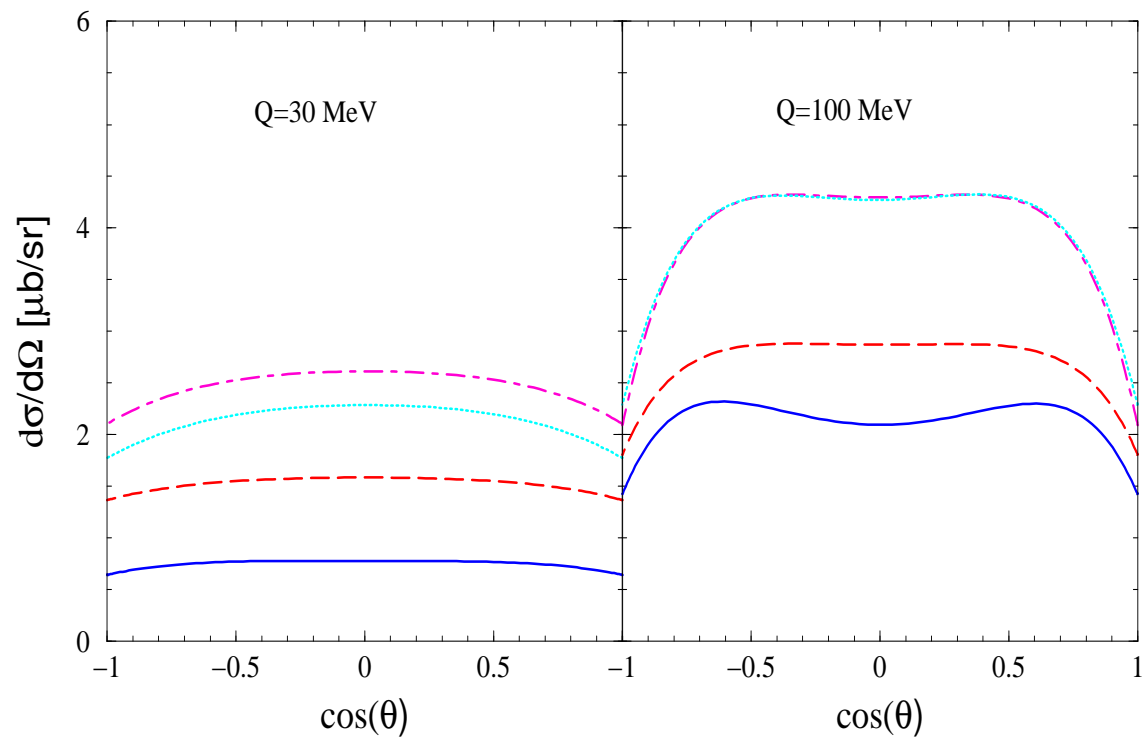


Fig. 6

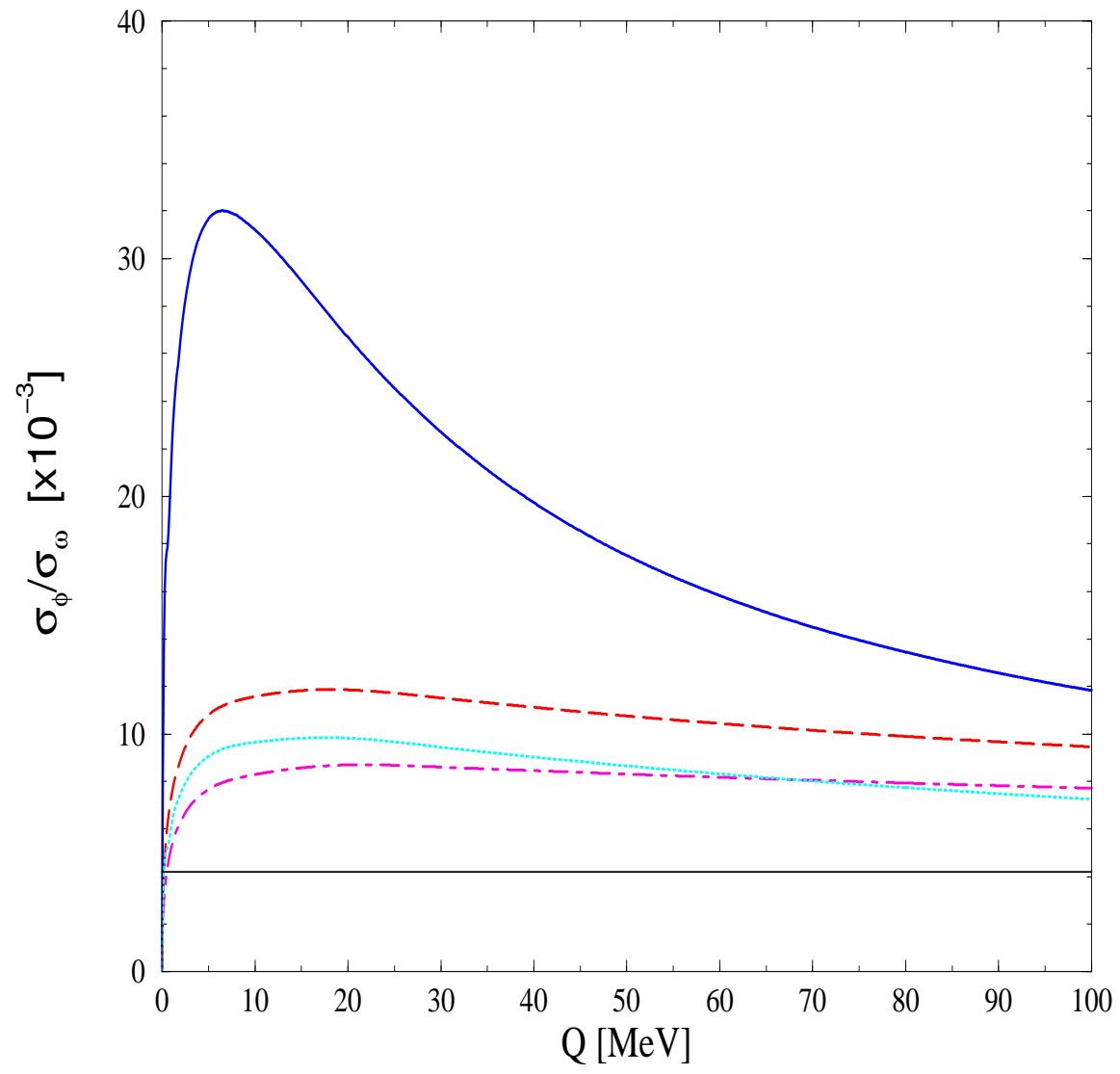


Fig. 7

